Stress relief during annealing of railway wheel steel characterized by synchrotron X-ray micro-diffraction

Stress relief during annealing of railway wheel steel characterized by synchrotron X-ray micro-diffraction

Yubin Zhang[1,*], Casey Jessop[2], Dimitrios Nikas[2,3], Tianbo Yu[1], Wenjun Liu [4] and Johan Ahlström[2,*]

[1] Department of Civil and Mechanical Engineering, Technical University of Denmark, 2800 Kgs. Lyngby, Denmark
[2] Department of Industrial and Materials Science, Chalmers University of Technology, 412 96 Gothenburg, Sweden
[3] Department of Engineering and Physics, Karlstad University, 651 88 Karlstad, Sweden
[4] Advanced Photon Source, Argonne National Laboratory, Argonne, 60439-4800 Illinois, USA

*E-mail: yubz@dtu.dk; johan.ahlstrom@chalmers.se

Abstract. Railway wheels in service experience rolling contact fatigue loading, but also need to resist frictional heating on braking, yielding temperatures up to 500 °C. The combination of mechanical and thermal loads leads to changes in the mechanical properties of the material. The focus of this study is to investigate the effect of annealing on local microstructure and residual stresses in railway wheel pearlitic steel (medium carbon steels, ~0.55 wt.% C) using synchroton X-ray Laue micro-diffraction. It is found that the local residual stress releases to a large extent after annealing at 500 °C. The stress formation and relief mechanisms and their relationship to the local microstructure are discussed.

1. Introduction

Medium carbon steels (with approximately 0.55 wt.% C) in railway wheel materials typically has a pearlitic microstructure with a small amount (5-10%) of pro-eutectoid ferrite decorating the previous austenite grain boundaries [1,2]. The manufacturing of railway wheels involves heat treatments in order to achieve desirable characteristics in mechanical properties and residual stress distributions. Investigations presented in literature show that the temperature in the wheel tread can rise to over 500 °C for wheels on block-braked freight trains [3]. The high temperatures reached during operation can, cause degradation of the microstructure, e.g. pearlite spheroidisation, which has been found to affect both the mechanical properties and fatigue behavior [2,4]. At the same time, the local residual stresses in the microstructure may relax. How the local residual stresses evolve upon annealing and how they may affect the degradation of the pearlite structure are essential information for optimization of the processing route and mechanical properties of railway pearlitic steel as well as for accurate constitutive modelling of the mechanical behaviour on different scales, and thus need to be quantified.

In this study, an advanced synchrotron X-ray technique, differential aperture X-ray microscopy (DAXM) [5,6], is used to quantify the changes in microstructure and residual plastic/elastic strain after annealing of the R8T steel grade used for railway wheels. This technique allows 3D non-destructive characterization of both crystallographic orientations and elastic strain with high precision (0.01° and 1×10^{-4}, respectively) [7]. By correlating the microstructural and strain changes upon annealing and comparing with other materials systems, the local stress relief mechanisms can be better understood.

2. Material and experimental procedures

The material studied in this investigation is the railway wheel steel R8T, which complies to the ER8 grade specified in the standard EN 13262-1 [8], and the specific batch examined in this work has a chemical composition as shown in Table 1. Samples were extracted from unused ('virgin') wheels approximately 15 to 20 mm below the wheel tread surface; this region is of interest since it becomes exposed to elevated temperatures and mechanical loading during operation. The typical microstructure of R8T steel in the selected position is shown in figure 1. The fraction of these so-called free ferrite grains is about 10%. The samples were annealed for 4 hours at temperatures at 300° C and 500 °C. More information about the samples can be found in [9].

Table 1. Chemical composition of R8T wheel material, in wt.%

C	Si	Mn	Mo	S	Cr	Ni	V	P	Fe
0.59	0.35	0.78	0.05	0.006	0.13	0.17	<0.005	0.005	Bal.

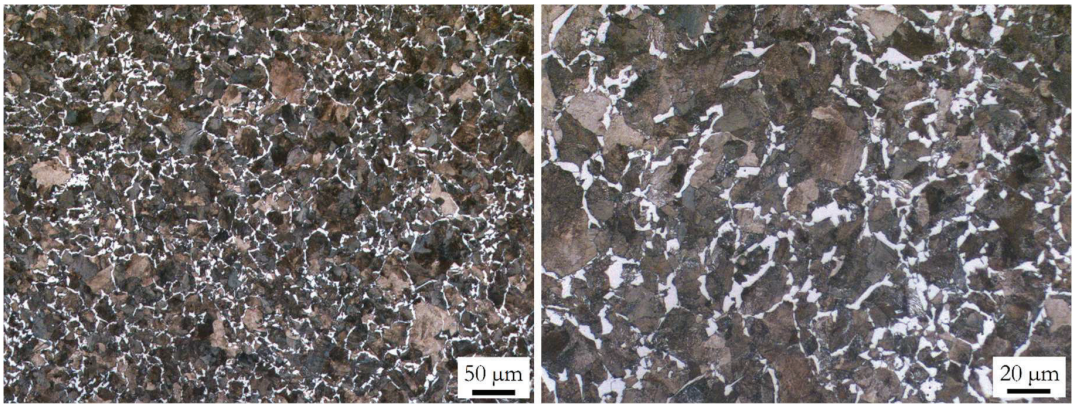

Figure 1. Optical micrograph of typical microstructure of R8T steel: free ferrite grains (white regions) and pearlite colonies (non-white regions).

2.1 Synchrotron X-ray diffraction

The DAXM experiments were conducted at beam line 34-ID-E at the Advanced Photon Source (APS), Argonne National Laboratory. First, a focused polychromatic microbeam (with size of ~0.3 µm) was used to determine the orientations of the grains. The X-ray microbeam scans the sample, which is mounted on a holder at an inclination angle of 45° to the incoming beam. A flat panel detector mounted in a 90° reflection geometry 510.3 mm above the specimen was used to record the Laue diffraction patterns. A Pt knife-edge, scanning along the sample surface at a distance of 250 µm, was used as a differential aperture for resolving diffraction patterns from different depths penetrated by the microbeam. The Laue patterns at each depth were reconstructed and indexed using the LaueGo software available at beamline 34-ID-E. More details about the experimental set-up can be found in [7].

A monochromatic beam was subsequently used for measurements of elastic strain within selected grains. By scanning the X-ray energy around the calculated value (calculated from the indexed Laue pattern using an ideal lattice parameter) for a selected Laue diffraction spot, the intensity distribution as

a function of the diffraction vector $Q = 2\pi/d$ (Q-distribution) can be determined for the selected diffraction spot at different depths. At each depth, the Q-distribution is fitted using a Gaussian function and the center of the distribution, Q_C, is used to determine the absolute lattice spacing, d. The elastic strain, ε, can then be determined using equation (1):

$$\varepsilon = \frac{(d-d_0)}{d_0} \quad (1)$$

where d_0 is the lattice spacing of the sample in the stress-free state. For the present study, d_0 was calculated, according to the chemical composition in table 1 with the lattice parameter $a_0 = 2.86734$ Å. More detailed information about the calculation procedure can be found in [10,11]. For the present study, the strain component along the normal direction of the polished surface was measured for three bulk grains for each sample.

3. Results

The microstructure of the annealed samples characterized using polychromatic beam DAXM are shown in figures 2 and 3. As can be seen from the inverse pole figure (IPF) maps (figures 2a and 3a), most of the volume within approximately 40 µm from the surface is indexed while the indexing rate is reduced at further depth. It is anticipated that the indexed grains are free ferrite grains and favorably oriented pearlite colonies, while the black areas most likely correspond to pearlite colonies, which cannot be indexed either due to unfavorable orientation of ferrite and shielding cementite lamellae, or due to large orientation gradients [4,9].

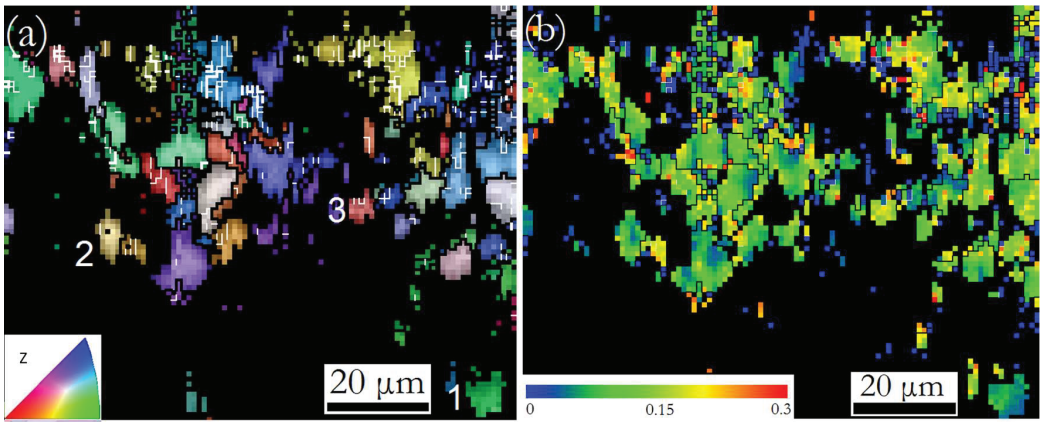

Figure 2. Distribution of crystallographic orientations in the sample annealed at 300 °C for 4h. (a) IPF map overlaid on top of a grey contrast from the number of indexed spots (in the range of 6-20), and (b) KAM map showing misorientation below 0.3° within the grains. The numbers 1-3 in (a) mark three grains selected for monochromatic energy scans. White and black lines in (a) mark boundaries with misorientations of >0.3° and 3°, respectively. (The sample surface is at the top of the figures)

The small misorientation range (0-0.3°) in the kernel average misorientation (KAM) map (figure 2b) emphasizes the local orientation variation within the free ferrite grains as well as in the ferritic phase of favorably oriented pearlite colonies. Such small misorientations would not be detected using 'standard' EBSD. The KAM value for a given pixel is defined as the average misorientation angle of that pixel to its 8 nearest neighbors, calculated with the proviso that misorientation angles above a cut-off angle (0.3° for this map) are not counted in the averaging process. The mean KAM value within the indexed ferrite grains selected from approx. 0.1 mm depth (to increase the chance that only free ferrite grains are included in the calculation) from sample surface is about 0.08° for both samples, which corresponds to a geometrically necessary dislocation (GND) density of 1.2×10^{13} m^{-2}, estimated using the method described in [12]. This result implies that there are no dramatic dislocation activities in the free ferrite grains in the temperature range 300-500°C.

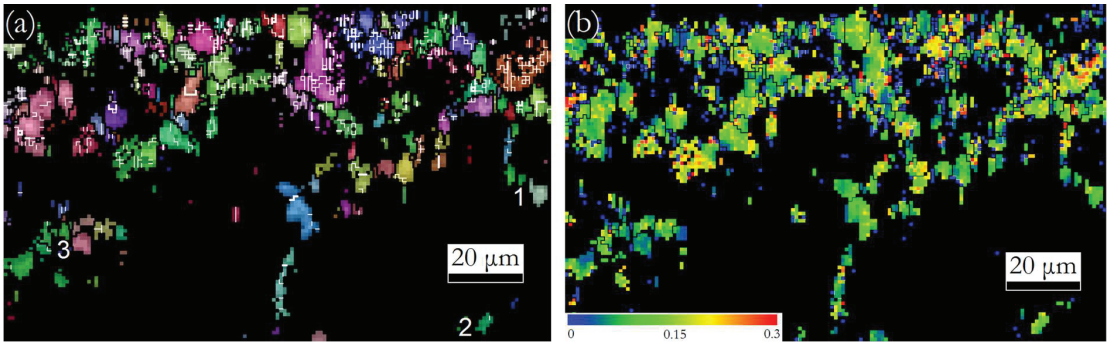

Figure 3. Distribution of crystallographic orientations in the sample annealed at 500 °C for 4h. (a) IPF map overlaid on top of a grey contrast from the number of indexed spots (in the range of 6-20), and (b) KAM map showing misorientation below 0.3° within the grains. The numbers 1-3 in (a) mark three grains selected for monochromatic energy scans. White and black lines in (a) mark boundaries with misorientations of >0.3° and 3°, respectively. (The sample surface is at the top of the figures)

In addition to the crystallographic orientation/misorientation information presented in the IPF and KAM maps, monochromatic energy scans were used to determine the elastic strain in certain grains in the samples annealed at 300 °C and 500 °C (numbered in figure 2a and figure 3a, respectively). The strains measured in three selected grains in each of the samples are shown in figure 4. The elastic strain values vary spatially within each grain and between grains, and therefore no systematic trend is seen to conclude if the strains close to the grain boundaries are higher or lower than those in the grain interiors. The overall strain variation is approximately 9×10^{-4} (from -5×10^{-4} to 4×10^{-4}) in the 300 °C annealed sample, and 3×10^{-4} (from -2×10^{-4} to 0.7×10^{-4}) in the 500 °C annealed sample. Despite the limited number of grains measured, it appears that a smaller reduced strain variation is observed as annealing temperature increases. The distribution of strains is narrower and the values are close to zero in the 500 °C annealed sample, indicating that the strain within the grains is largely released during the annealing. It is anticipated, based on the morphology and the ability to release residual stress at such low temperature (i.e. before severe spheroidisation occurs [9]), that these selected grains are free ferrite grains.

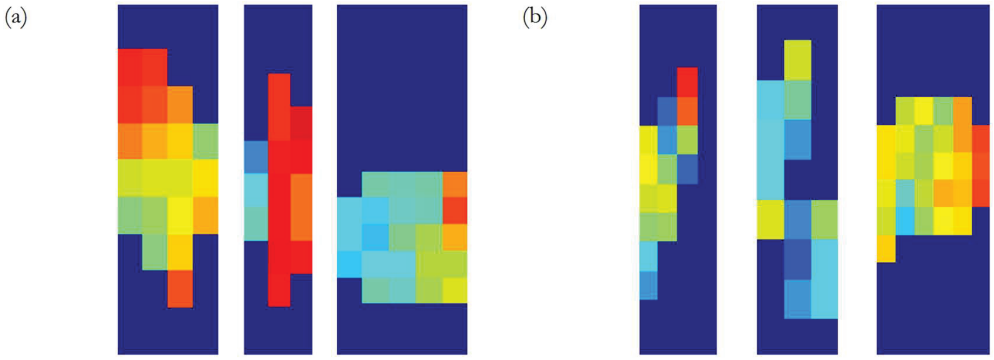

Strain (x10⁴)	Grain 1	Grain 2	Grain 3
Min.	-5.24	-2.43	-2.54
Max.	-1.67	3.94	1.43
Range	3.57	6.36	3.98

Strain (x10⁴)	Grain 1	Grain 2	Grain 3
Min.	-0.565	-0.650	-2.38
Max.	0.683	0.157	0.00572
Range	1.25	0.807	2.44

Figure 4. Strain range measured for 3 grains from samples annealed at (a) 300 °C, and (b) 500 °C. Note that the color scales are according to the minimum and maximum strain values, which are different for the different grains. All strains are $\times 10^{-4}$.

4. Discussion

The results show the relief of the local residual stresses in the present medium carbon R8T pearlitic steel up on annealing. The local residual elastic strain variation developed during manufacturing is 1.5-2×10^{-3} in the virgin material [13]. These residual strains/stresses are developed mainly during phase transformation because of the orientation and lattice differences between the ferrite and cementite [13,14]. Since the local orientation and size of the pearlite grains around individual free ferrite grains are different, the local residual stresses within and between individual free ferrite grains thus vary (see e.g. figure 4). The stress due to the thermal expansion seen in other steels [15] should be small in this material, as the thermal expansion coefficients for cementite and ferrite are similar in the temperature range 300-500 °C [16,17]. The present results show that the measured local residual stresses are largely released upon annealing at 500 °C, which further supports this argument, as thermal stresses are typically difficult to be removed.

Upon annealing at 300 °C, there is nearly no structural change in the pearlitic colonies [2,9]. A reduction of the GND density from 1×10^{14} m^{-2} [13] in the free ferrite grains in the virgin material to 1.2 ×10^{13} m^{-2} after annealing at 300 °C for 4h corresponds well to the reduction of elastic strain variation, from 1.5-2×10^{-3} to 9×10^{-4}. Upon annealing at the higher temperature of 500 °C, there is a further decrease in elastic strain in the free ferrite grains, although the GND density there is largely unchanged. At this stage, the stress relief should mainly be related to the recovery of the pearlitic colonies and the initial stages of spheroidization of the cementite [2,9].

The local residual strains/stresses in the present pearlitic steel can be compared with partially recrystallized pure iron [18], for a better understanding of the residual stress formation mechanisms. After annealing at 500-550 °C to ~10% recrystallization, a variation in residual elastic strain of 4×10^{-4} has been observed in the recrystallized grains of size in the range 5-25 μm. In those grains, the GND density is very low, in the order of 10^{-12} m^{-2}. The large difference in the GND density but similar variation in residual elastic strain between the iron and the present steel results suggests that the residual elastic strain variation within individual free/recrystallized ferrite grains is largely independent of GND density, but depends more on the surrounding pearlite colonies/deformed matrix of the steels. The development of medium- to long-range residual stresses from dislocation boundaries in deformed materials has been discussed and quantified extensively in the past (e.g. [19,20]). The presence of a significant residual stress variation in the free/recrystallized ferrite grains, with size significantly larger than the typical range affected by the long-range residual stresses from dislocation boundaries (0.5-1 μm) in the deformed materials, suggests that the formation mechanisms of long-range residual stresses have to be reconsidered taking the new results into account.

5. Summary

In the present study, the microstructure and elastic strain in annealed wheel steel samples were measured using differential aperture synchrotron X-ray microscopy. Only free ferrite grains and favorably oriented pearlite colonies with low orientation gradients were possible to index and it is difficult to differentiate between them in the region close to the surface, where indexing rates are high. A large variation in the elastic strain is seen within individual free ferrite grains as well as between free ferrite different grains. Both the local dislocation density and the residual stresses in the free ferrite grains decrease during annealing. The stress relief in the the free ferrite grains is mainly affected by the spheroidization of cementite in and recovery of the surrounding pearlitic colonies.

Acknowledgments

This work is part of the research activities within CHARMEC (Chalmers Railway Mechanics, www.charmec.chalmers.se). It was partly financed within the European Horizon 2020 research and innovation programme in the projects In2Track, In2Track2 and last in the In2Track3 project under grant agreement 101012456. YZ acknowledges the support by the Danish Council for Independent Research Fund (8022-00340B) and TY acknowledges the support by the European Research Council (ERC) under the European Union's Horizon 2020 research and innovation programme (grant No 788567, M4D). Use

of the Advanced Photon Source, an Office of Science User Facility operated for the U.S. Department of Energy (DOE) Office of Science by Argonne National Laboratory, was supported by the U.S. DOE under Contract No. DE-AC02-06CH11357.

References

[1] Cvetkovski K, Ahlström J and Karlsson B 2011 Monotonic and cyclic deformation of a high silicon pearlitic wheel steel *Wear* **271** 382–7
[2] Nikas D, Ahlström J and Malakizadi A 2016 Mechanical properties and fatigue behaviour of railway wheel steels as influenced by mechanical and thermal loadings *Wear* **366–367** 407–15
[3] Peters C J and Eifler D 2009 Influence of service temperatures on the fatigue behaviour of railway wheel and tyre steels *Mater. Test.* **51** 748–54
[4] Nikas D and Ahlström J 2014 Thermal deterioration of railway wheel steels *36th Riso international symposium of material science* pp 411–20
[5] Larson B C, Yang W, Ice G E, Budai J D and Tischler J Z 2002 Three-dimensional X-ray structural microscopy with submicrometre resolution *Nature* **415** 887–90
[6] Levine L E, Larson B C, Yang W, Kassner M E, Tischler J Z, Delos-Reyes M A, Fields R J and Liu W 2006 X-ray microbeam measurements of individual dislocation cell elastic strains in deformed single-crystal copper. *Nat. Mater.* **5** 619–22
[7] Larson B C and Levine L E 2013 Submicrometre-resolution polychromatic three-dimensional X-ray microscopy *J. Appl. Crystallogr.* **46** 153–64
[8] Anon 2009 *European standard for Wheels EN 13262 - Product requirements*
[9] Nikas D, Zhang Y, Jessop C and Ahlström J 2022 Effect of annealing on microstructure in railway wheel steel *IOP Conf. Ser. Mater. Sci. Eng. This conference.*
[10] Zhang Y B, Andriollo T, Fæster S, Liu W, Hattel J and Barabash R I 2016 Three-dimensional local residual stress and orientation gradients near graphite nodules in ductile cast iron *Acta Mater.* **121** 173–80
[11] Dhar S, Zhang Y, Xu R, Danielsen H K and Juul Jensen D 2017 Synchrotron X-ray measurement of residual strain within the nose of a worn manganese steel railway crossing *IOP Conference Series: Materials Science and Engineering* vol **219** p 012016
[12] Zhang Y and Barabash R 2019 High resolution mapping of orientation and strain gradients in metals by synchrotron 3D X-ray Laue microdiffraction *Quantum Beam Sci.* **3** 1–14
[13] Yildirim C, Jessop C, Ahlström J, Detlefs C and Zhang Y 2021 3D mapping of orientation variation and local residual stress within individual grains of pearlitic steel using synchrotron dark field X-ray microscopy *Scr. Mater.* **197** 113783
[14] Bramfitt B L and Marder A R 1973 A transmission-electron-microscopy study of the substructure of high-purity pearlite *Metallography* **6** 483–95
[15] Zhang Y B, Andriollo T, Fæster S, Barabash R, Xu R, Tiedje N, Thorborg J, Hattel J, Juul Jensen D and Hansen N 2019 Microstructure and residual elastic strain at graphite nodules in ductile cast iron analyzed by synchrotron X-ray microdiffraction *Acta Mater.* **167** 221–30
[16] Yershov V M 1981 High-Temperature X-Ray Investigation of Thermal Expansion of the Cementite Lattice. *Phys. Met. Metallogr.* **52** 90–4
[17] Bhadeshia H K D H 2020 Cementite *Int. Mater. Rev.* **65** 1–27
[18] Zhang Y, Yu T, Xu R, Thorborg J, Liu W, Tischler J Z, Godfrey A and Juul Jensen D 2022 Local residual stresses and microstructure within recrystallizing grains in iron *Submitted for Publication.*
[19] Levine L E, Geantil P, Larson B C, Tischler J Z, Kassner M E, Liu W, Stoudt M R and Tavazza F 2011 Disordered long-range internal stresses in deformed copper and the mechanisms underlying plastic deformation *Acta Mater.* **59** 5803–11
[20] Mughrabi H 1983 Dislocation wall and cell structures and long-range internal stresses in deformed metal crystals *Acta Metall.* **31** 1367–79